Nanostructured Platinum (H_I-ePt) Films: Effects of Electrodeposition Conditions on Film Properties

Joanne M. Elliott,* George S. Attard, Philip N. Bartlett, Nicholas R. B. Coleman, Daniel A. S. Merckel, and John R. Owen

Department of Chemistry, Southampton University, Southampton, United Kingdom, SO17 1BJ

Received June 11, 1999. Revised Manuscript Received September 16, 1999

A systematic investigation into the effects of deposition conditions on the electrochemical properties and nanostructure of high surface area (up to ∼460 $m^2\ cm^{-3}$) mesoporous platinum films (H_I-ePt) obtained by electroreduction of hexachloroplatinic acid (HCPA) from an hexagonal lyotropic liquid crystalline phase is reported. The surface area, repeat distance, and regularity of the nanostructure and the surface morphology of the films were shown to depend on the deposition conditions. In particular, the deposition potential was found to have a notable effect on the film surface area and on the uniformity of nanostructure. The results obtained are explained by variations in the efficiency of the deposition process and the relative contributions of competing reactions. Increasing the temperature of electrodeposition was found to increase significantly the surface areas of the films and to increase the repeat distance of the nanostructure. In addition, a roughening of the films on both a micro- and a nanometer scale was observed with an increase in temperature. We also found that the thickness of the electrodeposited films scaled linearly and that the volumetric surface area was constant, with the charge passed during the electrodeposition process, indicating uniform accessibility of the pore system.

Introduction

Over recent years materials with pore sizes in the mesoporous domain (2−50 nm according to the IUPAC convention)[1] have attracted considerable interest because of their potential applications in catalysis and chemical separations.[2−6] In 1992, it was shown that silica and aluminosilicates, having mesopores distributed on a spatially periodic long-ranged lattice, could be obtained by using cationic amphiphiles in formulations that were typically used in the hydrothermal syntheses of zeolitic materials.[2] The periodic porous architectures revealed by transmission electron microscopy suggested that the nanostructures in these materials (commonly denoted as MCM) were the result of one of the several liquid crystalline phases exhibited by the amphiphile acting as a template. It was subsequently shown that mesoporous oxides could be obtained at moderate temperatures and at atmospheric pressure by using a range of surfactants at concentrations that were above the critical micelle concentration, but typically less than 7 wt % with respect to the water content of the mixture.

In 1995, it was reported that each of the three liquid crystalline phases exhibited by the nonionic surfactant octaethylene glycol monohexadecyl ether ($C_{16}EO_8$) could be used to template silica with a nanostructure that is a direct cast of the supramolecular architecture of the phase in which it was formed.[7] These silicas were labeled H_I-SiO_2, $Ia3d$-SiO_2, and L_α-SiO_2. In contrast to the syntheses of the MCM mesoporous materials, the surfactant concentration used in these experiments was high, typically >30 wt %, to ensure that an homogeneous (i.e. single phase) liquid crystalline phase was obtained and that the topology of the phase remained unchanged throughout the progress of the reaction and the calcination process. We showed subsequently that the normal topology hexagonal (H_I) liquid crystalline phase could be used as a template for the synthesis of mesoporous platinum powders (H_I-Pt) via the reduction of HCPA.[5,8] This new type of platinum powder was characterized by a specific surface area of ∼60 $m^2\ g^{-1}$ (compared with 35 $m^2\ g^{-1}$ for platinum black), and large particle sizes (>100 μm). EXAFS data obtained from H_I-Pt were consistent with the platinum in the walls having a face-centered cubic packing, albeit with reduced coordination lengths.

Figure 1 depicts the 3D structure of an hexagonal liquid crystalline phase and the expected nanostructure of a material produced in its presence. Recently we reported the production of nanostructured platinum

* To whom correspondence should be addressed. E-mail: jme@soton.ac.uk

(1) Nettleship, I. *Key Eng. Mat.* **1996**, *122*, 305.
(2) Kresge, C. T.; Leonowicz, M. E.; Roth, W. J.; Vartuli, J. C.; Beck, J. S. *Nature* **1992**, *359*, 710.
(3) Beck. J. S. Ö. *J. Am. Chem. Soc.* **1992**, *114*, 10834.
(4) Attard, G. S.; Glyde, J. C.; Goltner, C. G. *Nature* **1998**, *378*, 366.
(5) Attard, G. S.; Goltner, C. G.; Corker, J. M.; Henke, S.; Templer, R. H. *Angew. Chem., Int. Ed. Engl.* **1997**, 36, *12*, 1315.
(6) Attard, G. S.; Bartlett, P. N.; Coleman, N. R. B.; Elliott, J. M.; Owen, J. R.; Wang, J. H. *Science* **1997**, *278*, 5339, 838.
(7) Attard, G. S.; Glyde, J. C.; Goltner, C. G. *Nature* **1995**, *378*, 366.
(8) Attard, G. S.; Coleman, N. R. B.; Elliott, J. M. *Stud. Surf. Sci. Catal.* **1998**, *117*, 89.

10.1021/cm991077t CCC: $18.00 © 1999 American Chemical Society
Published on Web 11/12/1999

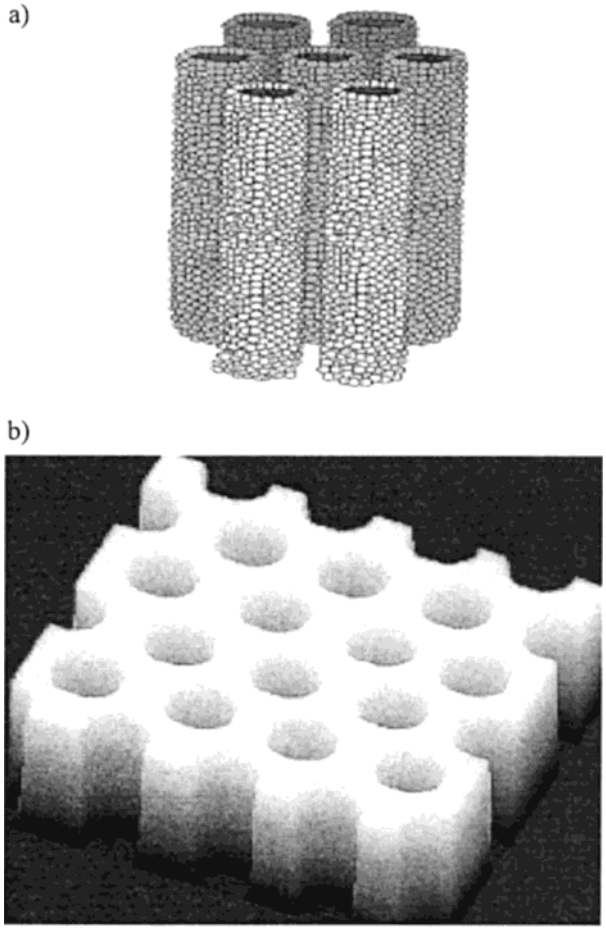

Figure 1. Schematic of (a) the 3D structure of an hexagonal liquid crystalline phase and (b) the expected nanostructure of a material produced in its presence.

films (H_I-ePt) by electrodeposition from an electroplating mixture which was in an H_I phase.[6] The resulting films were adherent and shiny, but were shown to have a nanostructure that was identical to that of the H_I-Pt powders.[8] This consisted of cylindrical pores distributed on an hexagonal lattice. For films from mixtures containing $C_{16}EO_8$, the pore diameter was found to be ~25 Å from transmission electron microscopy observations. The wall thickness at the point of nearest contact between neighboring pores was also found to be ~25 Å. From these structural parameters it was estimated that, on average, each film contained 4.62×10^{12} holes cm^{-2}. Initial studies also showed that the diameters of the pores could be controlled either by using surfactants with shorter or longer chains than $C_{16}EO_8$, or by swelling the phase with a hydrocarbon additive. Thus, for example, H_I-ePt with pore diameters ~18 Å could be obtained by using $C_{12}EO_8$ instead of $C_{16}EO_8$, while H_I-ePt with pore diameters of ~40 Å could be obtained from a quaternary mixture containing HCPA, water, $C_{16}EO_8$ and heptane, the latter in the molar ratio 1:1.

The specific surface area of an H_I-ePt film that has a geometrically perfect hexagonal nanostructure consisting of pores of diameter 25 Å and a pore to pore separation of 50 Å is predicted to be 21.94 $m^2\ g^{-1}$ (assuming that the platinum in the walls has a density of 21.4 g cm^{-3}); this is equivalent to a volumetric surface area of 360 $m^2\ cm^{-3}$. All results shown will be interpreted relative to this value. It is important to note that for a given nanostructure measurements of the specific or volumetric surface area should be independent of film thickness. In contrast, roughness factor values or double-layer capacitance values should increase proportionally with film thickness. Also it is to be expected that any changes in the pore to pore separation, regularity of the nanostructure, or surface roughness of a film will lead to significant changes in the surface area.

Electrochemical characterization of the H_I-ePt films using cyclic voltammetry and impedance spectroscopy has confirmed that they have high surface areas and concomitantly large double-layer capacitances. These properties, together with a uniform pore size distribution, mechanical stability, and ease of processing, suggest that metals electroplated from lyotropic phases could be of considerable interest for a wide range of applications (for example, in batteries, fuel cells, and sensors).[9−12] Although surfactants have often been reported as components of electroplating formulations, their use has been restricted to concentrations that are much lower than those required to form homogeneous lyotropic phases.[13] Hence, nothing is known about how the electrodeposition process variables might affect the properties of the films electrodeposited from liquid crystalline phases. In particular, the electroreduction of HCPA is not a simple one-step process but is a complex sequence of reactions and both the mass-transfer limitations and the kinetics of each step ultimately govern the amount of platinum deposited. Here we report on how the electrodeposition temperature, the deposition potential, and the amount of charge passed affect the properties of H_I-ePt films.

Experimental Section

Materials and Equipment. The surfactant, octaethylene glycol monohexadecyl ether ($C_{16}EO_8$) (98% purity), was purchased from Fluka, while hexacholoroplatinic acid hydrate (HCPA) (99.9% purity) was purchased from Aldrich. Both compounds were used as received. All solutions were prepared using deionized water, which was produced by passing tap water through a Whatman RO 50 water purification system. All glassware was cleaned by soaking in a 3% Decon 90 (Aldrich) solution for 24 h followed by rinsing with deionized water and drying in an oven at 50 °C. The electrochemical experiments were conducted on a purpose-built electrochemical workstation, using a conventional three-electrode system, comprised of a gold working electrode, a large surface area platinum gauze counter electrode, and a saturated calomel reference electrode (SCE), to which all potentials were referenced. The sample temperature was controlled to within ±0.1 °C of the set temperature over the range 25 to 85 °C by placing the sample in a Pyrex water-jacketed cell of volume ~3 cm^3, and using a Grant Y6 thermostated water bath to circulate water around the cell.

Liquid Crystalline Plating Mixture. The plating mixture used in these studies consisted of the ternary system $C_{16}EO_8$, HCPA, and water. A 1.9 M aqueous solution of HCPA was mixed with $C_{16}EO_8$ (50 wt %) in a capped vial at room temperature. A glass rod was employed for all manual mixing operations. On initial mixing of the components, the mixture

(9) Leroux, F.; Koene, B. E.; Nazar, L. F. *J. Electrochem. Soc.* **1996**, *143*, L181.
(10) Ye, S.; Vijh, A. K.; Dao, L. H. *J. Electrochem. Soc.* **1996**, *143*, L7.
(11) Pell, W. G.; Conway, B. E. *J. Power Sources* **1996**, *63*, 255.
(12) Wang, J.; Agnes, L. *Anal. Chem.* **1992**, *64*, 456.
(13) Kuhn, A. T. *Industrial Electrochemical Processes*; Elsevier: Amsterdam, 1971; p 336.

was opaque in appearance and had a creamy consistency. The opacity decreased and the mixture consistency became more gel-like on thorough mixing. At room temperature, a mixing period of ~10 min was needed to reach this stage. The vial was sealed and placed in a thermostated oven at ~45 °C for 10 min followed by vigorous shaking using a vortex mixer, this action was repeated until an homogeneous sample was obtained.

Investigation of the ternary mixture by polarized light microscopy revealed that the mixture formed an hexagonal phase that was stable to temperatures in excess of 90 °C.[14] These studies were conducted using an Olympus BH-2 polarized light microscope equipped with a Linkam TMS90 heating/cooling stage and a temperature control unit. The sample temperature could be maintained to within ±0.1 °C of the set temperature during the experiments. The hexagonal phase was identified on the basis of its optical texture, and the absence of new phases being formed when water was added to the mixture in penetration experiments indicated that this was a normal topology phase. Briefly, the penetration experiments required the preparation of a thin film of the mixture sandwiched between a coverslip and a glass slide. A drop of water was placed in contact with the coverslip such that capillary forces drew water to the sample. As the water penetrated the sample, a concentration gradient was established in the contact region. No phases other than the hexagonal phase were observed on the excess water side of the contact region, confirming that this phase was a normal topology phase.

Electrodeposition of H_I-ePt Films. Two types of working electrode were used depending on whether the electrodeposited films were to be used in electrochemical studies or in structural studies using electron microscopy. The H_I-ePt films used in the cyclic voltammetry studies were deposited onto gold wire electrodes of cross-sectional area varying from 7.85×10^{-7} to 0.071 cm^2 that were sealed either in glass or in epoxy resin (Struers Epofix Resin). Prior to use, each electrode was polished using Alumina (Buehler) in three grades: 25 μm, 1 μm, and 0.3 μm. Each electrode was then cleaned electrochemically by cycling in 2 mol dm^{-3} aqueous sulfuric acid between −0.2 V and +1.8 V vs SCE at a scan rate of 200 mV s^{-1}. This cycling process results in the sequential formation/removal of a layer of gold oxide at the electrode surface.[15] The large area H_I-ePt films used in the electron microscopy studies were deposited onto 1 cm^2 gold plate electrodes. These were prepared by evaporating a gold film (~200 nm thickness) onto glass with a thin (~7−8 nm) adhesive underlayer of chromium. Before use, these electrodes were cleaned by sonicating in propan-2-ol for 60 min. Both the wire and the large area electrodes were allowed to dry under ambient conditions before further use.

Electrodeposition of the platinum films was achieved under potentiostatic and thermostatic control; the potential was stepped from +0.6 V to growth potentials in the range +0.1 V to −0.4 V vs SCE. Postdeposition treatment of all films was identical. After deposition, the electrodes were removed from the cell and allowed to soak in ~5 cm^3 of water, which was regularly replaced, every 2 h (except overnight), for a period of 48 h. Films used in the TEM studies were allowed to dry for 3−4 h (under ambient conditions, in a covered container) before being scraped off directly onto supporting grids (carbon-coated copper grid, Agar Scientific Ltd). Films prepared for SEM analysis were snapped and imaged orthogonal to the cleavage plane in order to reveal the thickness of the electrodeposited film.

Electrochemical and Morphological Characterization of Platinum Films. The platinum films deposited on the gold wire electrodes were analyzed electrochemically by cycling in 2 mol dm^{-3} aqueous sulfuric acid between −0.2 V and +1.2 V vs SCE at a scan rate of 200 mV s^{-1}. The surface area of an electrodeposited film was determined by integrating the current passed during the forward and reverse cycles within the range +0.2 V to −0.2 V vs SCE, subtracting the charge associated with the double layer, halving the result (because the integration was carried out over both forward and reverse cycles), and finally converting to a surface area measurement (in units of squared centimeters), assuming a conversion factor of 210 μC cm^{-2}.[16] This surface area measurement was divided by the geometric area of the electrode to produce values of the roughness factor. The specific surface area of an H_I-ePt film was calculated from the deposition charge assuming a 75% faradaic deposition process efficiency (as determined by SEM studies).

Each electrode was also scanned between the limits −0.2 V and +1.2 V vs SCE at variable scan rates in the range 10−2000 mV s^{-1}. The current passed at +0.2 V vs SCE (anodic scan) was plotted versus the scan rate and the gradient of this straight line was taken to be the double-layer capacitance.

Electron Microscopy. Scanning electron micrographs were obtained using a JEOL JSM-6400 Scanning Electron Microscope operating at a voltage of 20 kV while the transmission electron micrographs were obtained using a JEOL 2000FX Transmission Electron Microscope operating at a voltage of 200 kV.

X-ray Diffraction. Low-angle X-ray diffractograms were recorded over the range ~0.7 to ~3.0 in 2θ degrees (Cu Kα radiation).

Results and Analysis

A typical cyclic voltammogram of a gold electrode recorded in 2 M sulfuric acid prior to electrodeposition is shown in Figure 2a. The cyclic voltammogram illustrates the expected behavior; peaks corresponding to the formation of a layer of gold oxide and its subsequent stripping are clearly visible.

Electroreduction of HCPA. Cyclic voltammograms were recorded between +0.6 V and −0.24 V vs SCE, at 25 °C, on an electrode of area 3.14×10^{-4} cm^2, at variable scan rate, in the lyotropic liquid crystalline mixture containing HCPA. Figure 2b shows the lower end of a cyclic voltammogram recorded at 10 mV s^{-1}; two reduction peaks, labeled "1" and "2" respectively, are visible at −0.15 V and −0.21 V vs SCE.

Deposition Potential. Potentiostatic deposition of platinum was carried out at +0.1, 0, −0.1, −0.2, −0.3, and −0.4 V vs SCE on an electrode of area 3.14×10^{-4} cm^2 (the temperature was controlled at 25 °C). After deposition and washing, the electrodes were analyzed by cyclic voltammetry in 2 M sulfuric acid. Figure 2c shows a typical example of a cyclic voltammogram for an H_I-ePt film, deposited at −0.1 V vs SCE (deposition charge density was 6.37 C cm^{-2}, deposition temperature was 25 °C, and the electrode area was 3.14×10^{-4} cm^2). The shaded area is assumed to relate to the double-layer region of the platinum, which is subtracted when the current associated with the hydrogen adsorption/desorption process is integrated for determination of the real surface area of the electrode. In this case the roughness factor of the electrode was determined to be 334. For comparison, a cyclic voltammogram of the gold electrode before deposition is included (dotted line), see also Figure 2a. The different amplitudes of the currents in these two voltammograms are clearly noticeable.

The surface area of the platinum deposit was found to vary significantly with the deposition potential.

(14) Attard, G. S.; Bartlett, P. N.; Coleman, N. R. B.; Elliott, J. M.; Owen, J. R. *Langmuir* **1998**, *14*, 26, 7340.

(15) Conway, B. E.; Angerstein-Kozlowska, H.; Hamelin, A.; Stoicoviciu, L. *Electrochim. Acta* **1986**, *31*, 1051.

(16) Trasatti, S.; Petrii, O. A. *J. Electroanal. Chem.* **1992**, *327*, 353.

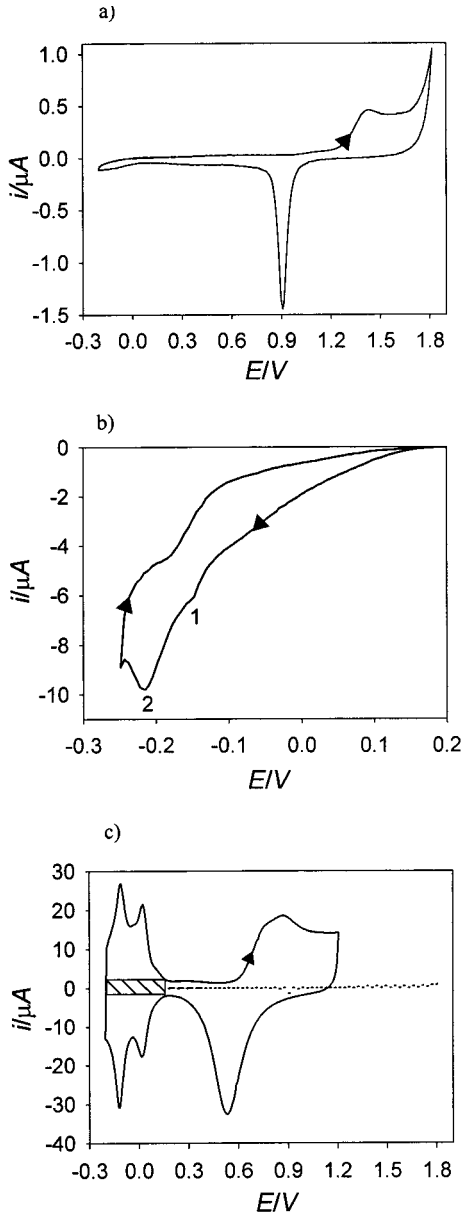

Figure 2. (a) Cyclic voltammogram for a gold electrode (3.14×10^{-4} cm^2 area) in 2 mol dm^{-3} aqueous sulfuric acid (aerobic conditions) at 200 mV s^{-1} between −0.2 V and +1.8 V vs SCE. (b) Cyclic voltammogram for a gold electrode (3.14×10^{-4} cm^2 area) in a 50% w/w octaethylene glycol monohexadecyl ether, 1.9 mol dm^{-3} aqueous HCPA mixture. Recorded at 25 °C at a scan rate of 10 mV s^{-1} between +0.6 V and −0.24 V vs SCE. (c) Cyclic voltammogram for a platinum film recorded in 2 mol dm^{-3} aqueous sulfuric acid (aerobic conditions) at 200 mV s^{-1} between −0.2 V and +1.2 V vs SCE. Deposition temperature was 25 °C, deposition charge density was 6.37 C cm^{-2}, deposition potential was −0.1 V vs SCE. Roughness factor is estimated to be 334.

Figure 3a shows how for a series of films deposited on an electrode, of area 3.14×10^{-4} cm^2, at a temperature of 25 °C with a charge density of 6.37 C cm^{-2}, the roughness factor varies with deposition potential. The highest roughness factor (∼570) was observed for films deposited at −0.2 V vs SCE. The capacitance of the system varied in the same manner, as shown in Table 1.

In addition, X-ray diffractograms for films deposited over this range of potentials were collected and are shown in Figure 3b,c. Films deposited at −0.1 V and above exhibited a sharp diffraction peak, corresponding to a repeat distance of ∼5.3 nm; however, films deposited at −0.2 V vs SCE exhibited only a broad diffraction peak and those deposited below −0.2 V vs SCE exhibited no peak at all. Since the efficiency of the deposition

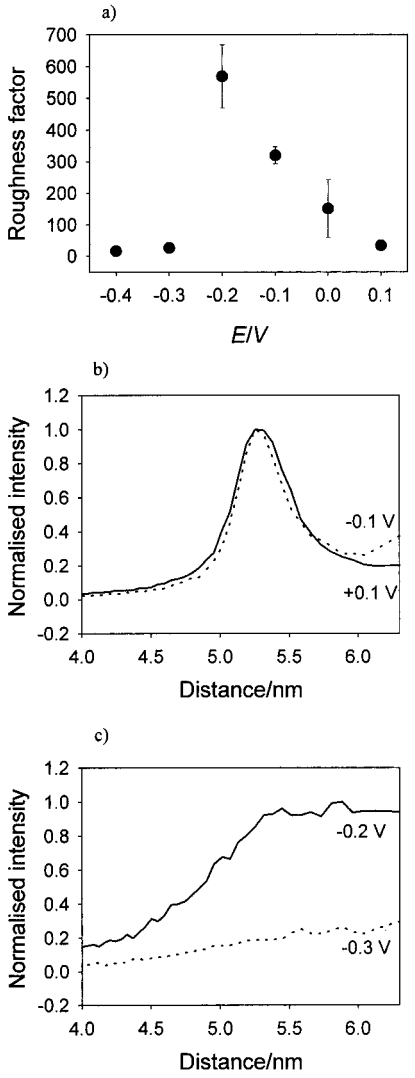

Figure 3. (a) Effect of deposition potential vs SCE on roughness factor. Error bars were calculated from the standard deviation of the data. In all cases the electrode area was 3.14×10^{-4} cm^2, deposition temperature was 25 °C, and deposition charge density was 6.37 C cm^{-2}. (b) X-ray diffractograms for platinum films deposited at 25 °C at various potentials. The dotted line represents data collected for platinum deposited at −0.1 V vs SCE, and the solid line represents data collected for platinum deposited at +0.1 V vs SCE. (c) X-ray diffractograms for platinum deposited at 25 °C at various potentials. The solid line represents data collected for platinum deposited at −0.2 V vs SCE, and the dotted line represents data collected for a platinum film deposited at −0.3 V vs SCE. The peaks occur at 5.3 nm.

Table 1. Variation in System Capacitance with Potential[a]

potential vs SCE, V	capacitance, μF cm^{-2}
+0.1	4 000
0	16 000
−0.2	60 000
−0.3	3 000
−0.4	2 000

[a] All values are determined for films of charge density 6.4 C cm^{-2}.

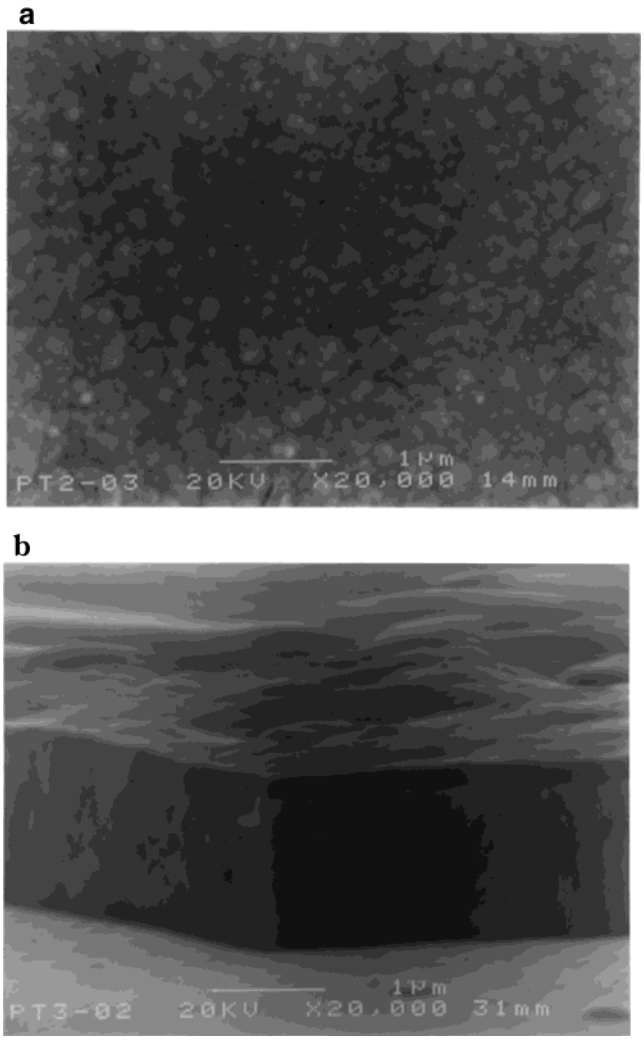

Figure 4. SEM images of nanostructured platinum deposited at −0.1 V vs SCE, deposition temperature was 25 °C and deposition charge density was ∼6.37 C cm^{-2}. Panel a represents the external surface morphology. Panel b represents a cross section through the electrode.

potential was also expected to vary with deposition potential, a series of platinum films were deposited on large area ∼1 cm^2 electrodes and the thickness of the resulting film was measured using SEM. Figure 4a shows the relatively flat and featureless surface morphology observed in SEM for films electrodeposited at −0.1 V vs SCE, at a temperature of 25 °C and with a charge density of 6.37 C cm^{-2}. Figure 4b shows a cross section of the platinum deposit; the actual film thickness was estimated to be ∼1500 nm. Further SEM analysis of films deposited at different potentials showed that the surface roughness increased substantially as the deposition potential was lowered and that the thickness of the platinum film also varied dramatically. The thickest films were obtained by deposition at −0.1 V and −0.2 V vs SCE. Either reducing or increasing the deposition potential away from this optimum resulted in a reduction in the thickness of the deposited layer.

The observed film thicknesses can be compared with the film thickness calculated for an ideal film exhibiting a perfect hexagonal nanostructure with pore diameters of ∼25 Å and ∼50 Å pore-to-pore distance. Platinum metal has a density of 21.4 g cm^{-3}, and since H_I-ePt with a perfect hexagonal nanostructure contains 77.3% (by volume) platinum and 22.7% (by volume) voids, the effective density of H_I-ePt is estimated to be ∼16.54 g cm^{-3}. Thus an H_I-ePt film deposited with a charge density of 6.37 C cm^{-2} and having a perfect hexagonal nanostructure would be expected to be 2000 nm thick, indicating that electrodeposition from the hexagonal liquid crystalline phase at −0.1 V vs SCE occurs with an approximate efficiency of 75%.

Table 2. Variation in System Capacitance and Film Thickness with Charge Density

charge density, C cm^{-2}	capacitance, μF cm^{-2}	charge density, C cm^{-2}	film thickness, nm
0.64	4 100	0.64	90
1.59	8 800	1.00	280
2.55	8 400	2.00	520
3.18	18 000	4.00	740
6.37	27 000a	6.37	1 490

[a] Denotes average of eight values, the 95% confidence interval was calculated as 27 000 ± 7 000 μF cm^{-2}.

This ideal model can only be applied to films deposited at potentials above −0.1 V vs SCE, because as the X-ray diffractograms in parts b and c of Figure 3 show only these films exhibit well-defined low-angle peaks, indicating the expected nanostructure. Figure 5 shows two typical TEM images obtained for films deposited at +0.1 V vs SCE, a regular ordered nanostructure is apparent.

TEM analysis was also carried out on films deposited at different potentials and confirmed that those deposited at −0.1 V vs SCE and above had a regular nanostructure, those deposited at −0.2 V vs SCE exhibited a disordered nanostructure, and those deposited below −0.2 V vs SCE had no observable nanostructure.

By taking the efficiency of the deposition process into account it was possible to calculate the volumetric surface area and the specific surface area of the platinum deposits. The value for films deposited at −0.1 V vs SCE was calculated as 238 m^2 cm^{-3}, for convenience it should be noted that this value is equivalent to 14.38 m^2 g^{-1}. These parameters are easily interconverted and for simplicity only the volumetric surface area will be quoted in further examples.

Deposition was also carried out on electrodes of different size, that is, with diameters varying from 10 μm up to 3 mm. Cyclic voltammetric analysis of the platinum films showed that for electrodes with areas greater than 3.14 × 10^{-4} cm^2 (200 μm diameter) the roughness factor was constant, see Figure 6. However, as the size of the electrode decreased further the roughness factor also appeared to decrease.

Charge Density. As expected the volumetric surface area of the films was constant with deposition charge density. The value was constant at 238 m^2 cm^{-3}. The double-layer capacitance was found to vary linearly with charge density as shown in Table 2. The linear increase in film thickness as observed in SEM is also shown in Table 2.

Electrodeposition Temperature. Films were deposited at several temperatures over the range 25−85 °C, at −0.1 V vs SCE with a charge density of 6.37 C cm^{-2} onto an electrode of area 3.14 × 10^{-4} cm^2. A stable H_I phase was present over this temperature range as

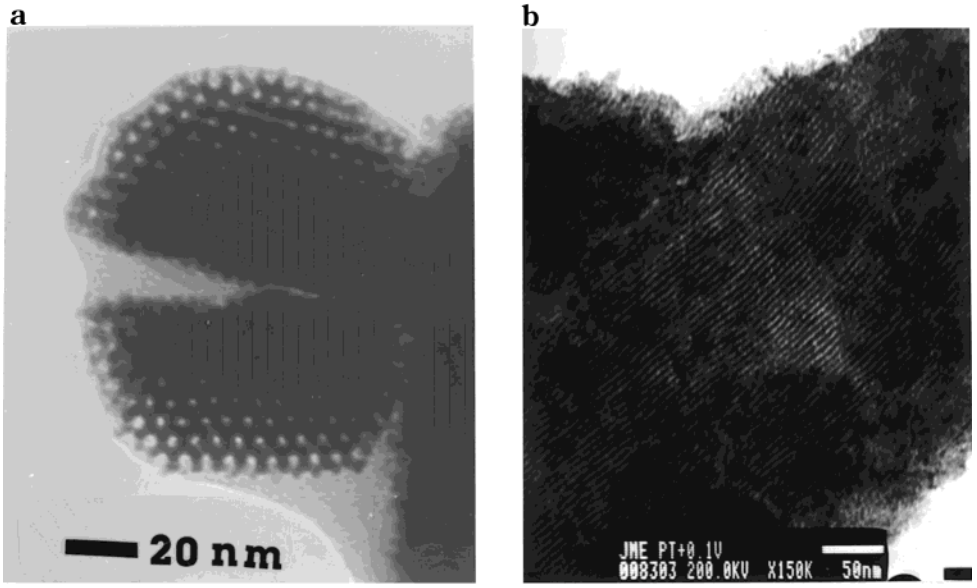

Figure 5. TEM images of nanostructured platinum deposited at +0.1 V vs SCE and at 25 °C. Panel a represents a view of the pores end on. Panel b represents a side view of the pores. Films were deposited with a charge density of ~ 6.37 C cm^{-2}.

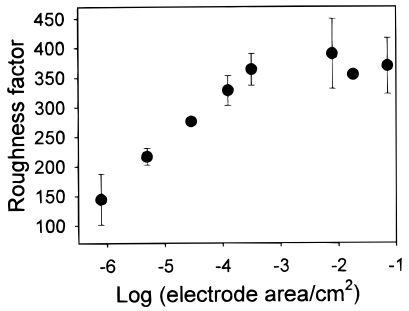

Figure 6. Effect of electrode area upon roughness factor. Error bars were calculated from the standard deviation of the data. In all cases the deposition charge density was 6.37 C cm^{-2}, the deposition temperature was 25 °C, and the deposition potential was −0.1 V vs SCE.

Table 3. Variation in Film Thickness with Temperature

T, °C	film thickness, nm per C cm^{-2}
25	235 ± 60 (n = 6)[a]
35	160
65	195
65	230
75	195

[a] Denotes average of six values, the 95% confidence interval was calculated as 233 ± 60 nm per C cm^{-2}.

confirmed by polarized light microscopy.[14] Table 3 shows that constant film thicknesses were observed with increase in deposition temperature, hence deposition efficiency remained the same at ~75%.

The SEM images illustrated in parts a and b of Figure 7 show the surface morphology of a platinum film deposited at 65 °C, comparing Figure 7a with Figure 4a shows the dramatic effect deposition temperature has upon film roughness. The volumetric surface area of the films was calculated, on the basis of an efficiency of 75%, and is shown in Figure 8a; the dotted line shows the value calculated for an ideally nanostructured film.

(17) Bard, A. J.; Parsons, R.; Jordan, J. *Standard Potentials in Aqueous Solutions*; Marcel Dekker: New York, 1985.

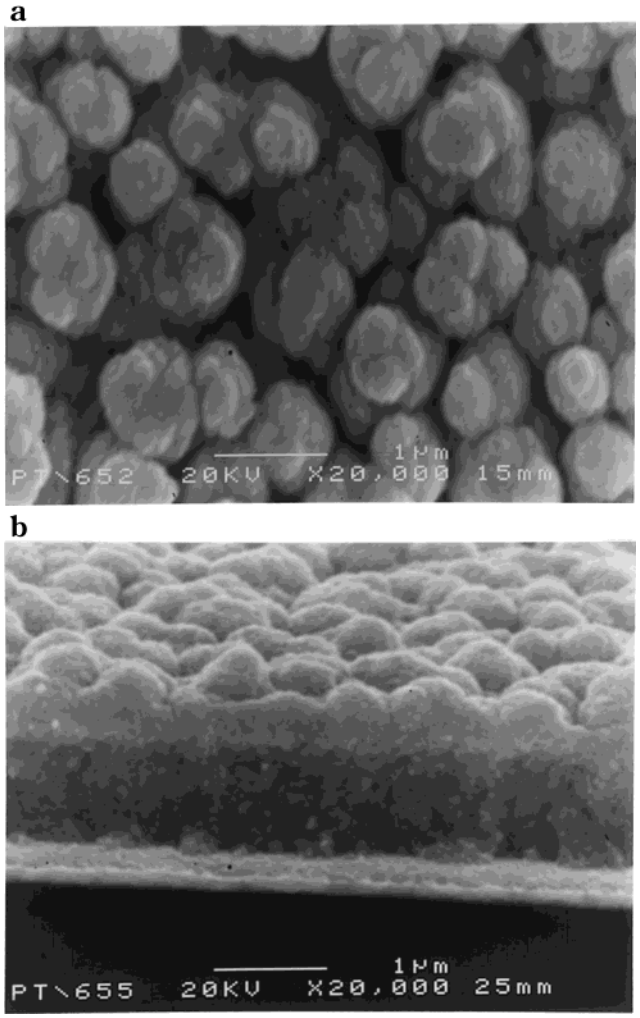

Figure 7. SEM images of nanostructured platinum deposited at −0.1 V vs SCE, deposition temperature was 65 °C and deposition charge density was ~6.37 C cm^{-2}. Panel a represents the external surface morphology. Panel b represents a cross section through the electrode.

The same model was applied to all films although the repeat distance of the nanostructure was shown to

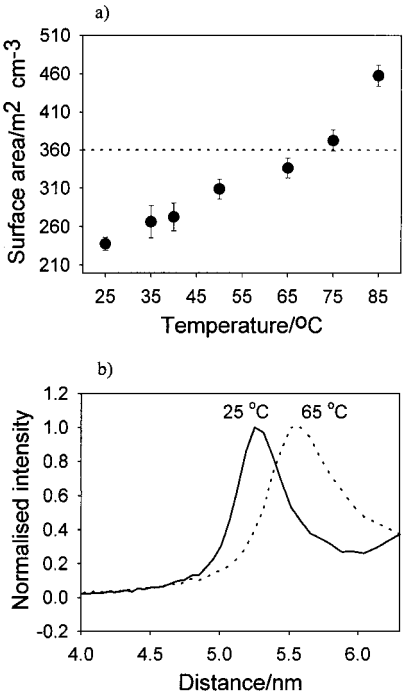

Figure 8. (a) Effect of deposition temperature upon volumetric surface area of platinum deposits, area of electrode was 3.14×10^{-4} cm^2. Error bars were calculated from the standard deviation of the data. The dotted line represents the value of the volumetric surface area of an ideal nanostructure. In all cases the deposition charge density was 6.37 C cm^{-2} and the deposition potential was −0.1 V vs SCE. (b) X-ray diffractograms for platinum films deposited at different temperatures. The solid line represents data collected for a platinum film deposited at 25 °C, the peak occurs at 5.3 nm, and the dotted line represents data collected for a platinum film deposited at 65 °C, the peak occurs at 5.6 nm.

increase slightly as deposition temperature was increased; see Figure 8b. The X-ray diffractograms were obtained for films deposited at both 25 and 65 °C. Although both films exhibited low-angle diffraction peaks, the spacing was found to increase from 5.3 to 5.6 nm with increasing deposition temperature. In addition, the half-height peak width was greater for the higher temperature deposit, indicating that the system was more disordered.

TEM analysis was also carried out on films deposited at higher temperatures and showed that although a nanostructure was present the inner walls of the pore structure were quite rough.

At 25 °C the volumetric surface area of the films was less than that calculated for a film with a geometrically perfect nanostructure; however, as the deposition temperature was increased the volumetric surface area of the films increased, tending toward the value calculated for an ideally nanostructured film and eventually rising above it. A linear relationship was observed for the double-layer capacitance as shown in Table 4.

Discussion

In all cases cyclic voltammetry of the electrodeposited platinum films in sulfuric acid showed fine structure in the hydride adsorption/desorption region which is characteristic of polycrystalline platinum. However, using lyotropic liquid crystals as templating agents is seen to produce films with highly ordered well-controlled

Table 4. Variation in System Capacitance with Temperature

T, °C	capacitance, μF cm^{-2} [a]
35	34 000
40	36 000
50	40 000
65	42 000
75	56 000
85	54 000

[a] All values were determined for films of charge density 6.4 C cm^{-2}.

porosity only when the electrodeposition conditions are controlled to eliminate unwanted side reactions. Films exhibiting a well-defined and ordered nanostructure, that is, an array of pores situated on an hexagonal lattice were observed only when deposition was carried out at −0.1 V vs SCE and above. The inner walls of the pore structure were quite rough and a side view of the hexagonal nanostructure indicated that the channels extended over a range of at least several hundred nanometers. The channels were not straight and a degree of meandering was observed. As the deposition temperature was increased the nanostructure became less ordered.

The electrodeposition process was found to be complex. It has been suggested that the electrodeposition of platinum from HCPA may involve two redox processes:

$$PtCl_6^{2-} + 2e^- \leftrightarrow PtCl_4^{2-} + 2Cl^- \qquad E° = 0.726 \text{ V vs NHE}^{17}$$

$$PtCl_4^{2-} + 2e^- \leftrightarrow Pt + 4Cl^- \qquad E° = 0.758 \text{ V vs NHE}^{17}$$

The current potential curves for the platinum electrodeposition process (Figure 2b) shows two waves, supporting the participation of $PtCl_4^{2-}$ in the deposition process.[18] In addition, the roughness factor of the platinum films was found to decrease as the size of the electrodes used was reduced, indicating that the efficiency of the deposition process was decreasing. As the electrodes become smaller more efficient radial diffusion of the intermediate Pt^{2+} species away from the electrode surface occurs before reduction to platinum metal can take place and the deposition efficiency is decreased.

Estimation of the efficiency of the deposition process requires the comparison of the electrodeposited films with an ideal nanostructured film of repeat distance ~5.0 nm. As the X-ray diffraction peaks in Figures 3b, 3c, and 8b show, the quality of the nanostructure is variable depending on the exact condition present during film deposition. Thus estimates of the efficiency of the process are expected to be meaningful only for films exhibiting close to ideal nanostructures, i.e., when deposition was carried out at −0.1 V vs SCE and above.

The highest roughness factors were obtained for films deposited at −0.2 V vs SCE; this was due to a high degree of roughness in the surface morphology of the film in combination with a disordered porosity. The nonlinear change in roughness factor as the deposition potential was lowered from +0.1 V to −0.2 V vs SCE is

(18) Georgolios, N.; Jannakoudakis, D.; Karabinas, P. *J. Electroanal. Chem.* **1989**, *264*, 235.

due to an increase in the efficiency of the deposition process. Indeed film thickness did increase as the deposition potential was lowered from +0.1 V to −0.2 V vs SCE. However, films produced at −0.2 V vs SCE were of the same thickness as those produced at −0.1 V vs SCE, indicating that in this case the deposition efficiency was the same. Although the external surface roughness of the film was found to increase upon reducing the deposition potential from +0.1 V to −0.2 V vs SCE, this factor alone cannot account for the large change observed in specific surface area. It is suggested that side reactions such as the evolution of gas at the electrode/electrolyte interface (a feasible process at the surface of platinum electrodes held at these potentials) led to the disruption of the nanostructure, as supported by TEM and X-ray diffraction measurements. Hence films deposited at −0.2 V vs SCE exhibited even greater surface areas due to increased accessibility of the pore system as a direct result of the disordered nanostructure.

When the deposition potential was decreased further to −0.3 and −0.4 V vs SCE a sharp decrease in the specific surface area was observed. This effect was due to the increasing domination of competing reactions such as proton reduction. These competing reactions would reduce the deposition efficiency significantly; hence thinner films were obtained at these lower potentials. Severe hydrogen evolution at these lower potentials would also lead to the observed roughening of the surface of the films and to the loss of nanostructure, as supported by TEM and X-ray diffraction measurements. The same principles can be used to explain the trends in system capacitance observed for films deposited over this range of potentials.

The fact that the observed volumetric surface area for films deposited at 25 °C is lower than the theoretical value but tends toward the value calculated for an ideally nanostructured film as deposition temperature was increased could be a consequence of the films containing areas of nanostructure not accessible by the electrolyte. The volumetric surface area of the films was found to be constant with deposition charge density, suggesting that a fixed proportion of the platinum films be inaccessible to electrolyte over the range of film thickness studied. However, as the deposition temperature was increased the nanostructure became less perfect and defects were introduced, supported by TEM and X-ray diffraction measurements. These defects correspond to holes connecting adjacent cylindrical pores and would effectively open up the structure and increase accessibility. The roughening of the nanostructure at high temperatures would explain why the real surface area of the system is greater than that calculated for an ideal nanostructured system.

X-ray diffraction and TEM analysis of the films were found to complement one another. TEM analysis has the advantage that it allows the nanostructure to be observed directly. However, drawbacks associated with this method are that only a relatively small proportion of the sample can be analyzed and it can be very difficult to determine accurate repeat distances, given the electron dense nature of platinum. X-ray diffraction provides an alternative route to determining the relative order of the nanostructure and its repeat distance. To convert the real surface area measurements into useful volumetric or specific surface area measurements it was necessary to be able to take the efficiency of the deposition process into account. SEM studies provided a valuable preliminary indication of the efficiency of the deposition process; however, variations in the uniformity of the nanostructure meant that not all films could be compared in this way. A more accurate method of determining the deposition efficiency in future studies may be to use an Electrochemical Quartz Crystal Microbalance (EQCM).

Conclusions

The results we have described show that it is possible to prepare high surface area (up to 460 m^2 cm^{-3}) platinum films by deposition from a lyotropic liquid crystalline phase. An important point is that the films are very smooth and are strongly adhered to the electrode surface. We have found that temperature, and deposition potential can lead to significant changes in the specific surface area, nanostructure, and macroscopic morphology of the films. We have shown that it is possible to produce platinum films with a high surface area under a variety of conditions either by deposition at −0.2 V vs SCE or at high temperatures. However, films with the most ordered nanostructure are produced only when the conditions are carefully controlled within a set range of parameters, that is, at deposition potentials greater than −0.1 V vs SCE and at 25 °C. Our studies highlight the importance of conducting systematic studies of the effect of electrodeposition conditions on film properties to determine the process parameters required to produce films that are tailored to specific applications.

Acknowledgment. The authors would thank B. Cressey and M. Ghanem for assistance with TEM and X-ray diffraction studies, respectively. This work was supported by the UK Engineering and Physical Science Research Council.

CM991077T